Caveolin limits membrane microdomain mobility and integrin-mediated uptake of fibronectin-binding pathogens

Christine Hoffmann[1,*], Anne Berking[1,*], Franziska Agerer[2,‡], Alexander Buntru[1], Florian Neske[2,§], G. Singh Chhatwal[3], Knut Ohlsen[4] and Christof R. Hauck[1,¶]

[1]Lehrstuhl Zellbiologie X908, Universität Konstanz, Universitätsstr. 10, 78457 Konstanz, Germany
[2]Zentrum für Infektionsforschung, Universität Würzburg, 97080, Germany
[3]Helmholtz Zentrum für Infektionsforschung, Braunschweig, 38124, Germany
[4]Institut für Molekulare Infektionsbiologie, Universität Würzburg, 97080, Germany

*These authors contributed equally to this work
‡Present address: Nexigen GmbH, Ludwig-Erhard-Allee 2, 53175 Bonn, Germany
§Present address: Paul-Ehrlich-Institute, Department of Virology, Paul-Ehrlich-Str. 51-59, 63225 Langen, Germany
¶Author for correspondence (christof.hauck@uni-konstanz.de)

Accepted 20 August 2010
Journal of Cell Science 123, 4280-4291

doi:10.1242/jcs.064006

Summary

Staphylococcus aureus, which is a leading cause of hospital-acquired infections, binds via fibronectin to integrin α5β1, a process that can promote host colonization in vivo. Integrin engagement induces actin cytoskeleton rearrangements that result in the uptake of *S. aureus* by non-professional phagocytic cells. Interestingly, we found that fibronectin-binding *S. aureus* trigger the redistribution of membrane microdomain components. In particular, ganglioside GM1 and GPI-linked proteins were recruited upon integrin β1 engagement, and disruption of membrane microdomains blocked bacterial internalization. Several membrane-microdomain-associated proteins, such as flotillin-1 and flotillin-2, as well as caveolin, were recruited to sites of bacterial attachment. Whereas dominant-negative versions of flotillin-2 did not affect bacterial attachment or internalization, cells deficient for caveolin-1 (*Cav1*$^{-/-}$) showed increased uptake of *S. aureus* and other Fn-binding pathogens. Recruitment of membrane microdomains to cell-associated bacteria was unaltered in *Cav1*$^{-/-}$ cells. However, fluorescence recovery after photobleaching (FRAP) revealed an enhanced mobility of membrane-microdomain-associated proteins in the absence of caveolin-1. Enhanced membrane microdomain mobility and increased uptake of *S. aureus* was repressed by expression of wild-type caveolin-1, but not caveolin-1 G83S, which harbors a point mutation in the caveolin scaffolding domain. Similarly, chemical or physical stimulation of membrane fluidity led to increased uptake of *S. aureus*. These results highlight a crucial role for caveolin-1 in negative regulation of membrane microdomain mobility, thereby affecting endocytosis of bacteria-engaged integrins. This process might not only limit host cell invasion by integrin-binding bacterial pathogens, but might also be physiologically relevant for integrin-mediated cell adhesion.

Key words: Caveolin, Endocytosis, Fibronectin, Integrin, Lipid rafts, Staphylococci

Introduction

Pathogenic bacteria and viruses use various endocytic pathways and receptors to enter host cells (Pizarro-Cerda and Cossart, 2006). One major group of eukaryotic receptors involved in the uptake of pathogens are integrins, heterodimeric glycoproteins, which have an important role in different cellular processes such as cell adhesion, migration and proliferation (Hynes, 2002; van der Flier and Sonnenberg, 2001). Although the primary role of most integrins is to connect cells with the extracellular matrix (ECM) or with neighboring cells, they can also mediate endocytotic processes. Classical studies have demonstrated that under steady-state conditions in adherent CHO cells, about 10–15% of the fibronectin receptor cycles between an endocytic compartment and the cell surface within 10 minutes (Bretscher, 1989). Steady-state endocytosis of integrins seems to occur in the absence of a ligand and involves the clathrin-dependent endocytosis machinery (Caswell and Norman, 2008). In addition to an endocytotic recycling of unoccupied receptors, integrins are involved in the uptake of ligands. There are dedicated phagocytotic integrins, such as integrin αMβ2 (complement receptor 3), that internalize particulate material (Dupuy and Caron, 2008). Furthermore, integrin αvβ3, the collagen-binding integrin α2β1, and the fibronectin-binding integrin α5β1 are taken up together with their ligands, thereby contributing to the turnover of the extracellular matrix (Lee et al., 1996; Memmo and McKeown-Longo, 1998; Shi and Sottile, 2008).

Several pathogenic bacteria exploit this endocytotic capacity of integrins to promote internalization by non-professional phagocytes (Hauck et al., 2006). Bacterial proteins such as the *Yersinia enterocolitica* Invasin directly bind to integrins and, upon receptor clustering, induce a zipper-style uptake mechanism that involves integrin-associated protein tyrosine kinase signaling and reorganization of the actin cytoskeleton (Alrutz and Isberg, 1998; Dersch and Isberg, 1999). By contrast, other microbes have evolved ECM-binding proteins, which they use to immobilize integrin ligands on their surface (Boyle and Finlay, 2003). Gram-positive bacteria such as *Staphylococcus aureus* and *Streptococcus pyogenes* express cell-wall-anchored fibronectin-binding proteins (FnBPs or Sfb1, respectively), which can capture soluble fibronectin (Hauck and Ohlsen, 2006). An extended protein–protein interaction between repeats in the bacterial adhesin and the type I modules of fibronectin secures the ECM protein on the bacterial surface (Schwarz-Linek

et al., 2003). Bacteria-bound fibronectin exposes the tripeptide RGD motif within the tenth fibronectin type III module, which allows association with cellular integrins. Thereby, these pathogens use the physiological ligand to connect to integrin α5β1 (Fowler et al., 2000; Sinha et al., 1999). Upon engagement of integrin α5β1, fibronectin-coated bacteria trigger recruitment of integrin-associated proteins and activate tyrosine kinases such as focal adhesion kinase (FAK) and Src (Agerer et al., 2005; Agerer et al., 2003; Fowler et al., 2003; Ozeri et al., 2001). In contrast to *Yersinia* Invasin-mediated internalization, ultrastructural analysis of the uptake of fibronectin-coated streptococci or staphylococci reveals only minor cell protrusions that could be involved in a zipper-style uptake (Agerer et al., 2005; Rohde et al., 2003). Moreover, large invaginations are formed beneath the fibronectin-coated bacteria, and immunofluorescence and transmission electron microscopy suggests that caveolin-containing membrane microdomains are involved in the uptake process (Agerer et al., 2005; Rohde et al., 2003).

Recently, the endocytosis and turnover of fibronectin via integrin α5β1 has been linked to caveolin-1 and has been shown to occur in a clathrin-independent manner (Shi and Sottile, 2008; Sottile and Chandler, 2005). Earlier investigations in T lymphocytes had suggested that upon ligand binding, integrins move into a cholesterol- and ganglioside-rich membrane fraction and converge with membrane regions containing GPI-anchored proteins (Leitinger and Hogg, 2002; van Zanten et al., 2009). In turn, activation of integrins also results in accumulation of ganglioside GM1 and increases membrane order (del Pozo et al., 2004; Gaus et al., 2006) suggesting that ligand-bound integrins are able to locally influence the lipid composition of their membrane microenvironment. However, it is currently unknown whether fibronectin-coated bacteria induce changes in the organization of the host cell membrane and whether such alterations have a functional role for the integrin-mediated endocytosis of the bacteria.

Therefore, we analyzed the distribution of membrane microdomains upon contact of fibronectin-binding *S. aureus* to host integrins. Engagement of integrins by fibronectin-coated bacteria or recombinant bacterial adhesins led to a local accumulation of membrane microdomains, and cholesterol depletion reduced integrin-initiated uptake of the bacteria. Surprisingly, genetic deletion or RNAi-mediated knockdown of caveolin-1 strongly enhanced internalization of bacteria. Caveolin-1-deficient cells exhibited increased mobility of membrane microdomain components that correlated with increased bacterial uptake and that was reverted by expression of the wild type, but not a scaffolding-domain mutant of caveolin-1. Furthermore, physical or chemical enhancement of membrane microdomain mobility increased the internalization of *S. aureus* in the presence of caveolin. Together, our results not only demonstrate a functional role for cholesterol-rich membrane microdomains in bacterial internalization, but also reveal a crucial contribution of caveolin-1 to limiting membrane mobility and endocytosis of ligand-occupied integrins.

Results

Attachment of *S. aureus* to host cells induces the redistribution of membrane microdomains

Integrins have been implicated in the organization of ganglioside-rich and caveolin-positive microdomains in the plasma membrane. In particular, integrin binding to the extracellular matrix influences the distribution of ganglioside GM1 and increases local membrane order (del Pozo et al., 2004; Gaus et al., 2006). To investigate whether integrin engagement by fibronectin-binding *S. aureus* alters the distribution of membrane components in mammalian cells, mouse fibroblasts were infected for 2 hours with either Rhodamine-labeled *S. aureus* (strain Cowan) or with the non-fibronectin-binding species *S. carnosus*. Following infection, the fixed samples were stained with the FITC-coupled cholera toxin B-subunit (CT–FITC), which selectively binds to ganglioside GM1. A pronounced local accumulation of GM1 was observed in the vicinity of cell-attached *S. aureus*, but not *S. carnosus* (Fig. 1A). Quantification of the fluorescence signals showed that GM1 was highly enriched within a 1–2 μm distance surrounding the bacteria (Fig. 1A). In contrast to the strong recruitment of GM1, the ganglioside Gb3, which was visualized by the shiga toxin B-subunit (Sandvig et al., 1993), was only found occasionally in the vicinity of cell-associated staphylococci (supplementary material Fig. S1), suggesting recruitment of particular subsets of membrane microdomains to adherent bacteria.

Ganglioside- and cholesterol-rich membrane microdomains are also enriched for GPI-anchored proteins (for a review see Kinoshita et al., 2008). Indeed, a pronounced recruitment of a GPI-anchored green fluorescent protein (GPI–GFP) to cell-attached *S. aureus* was observed (Fig. 1B). Recruitment of GM1 required host cell integrin β1, because accumulation of GM1 around cell-associated bacteria was not observed when integrin-β1-deficient mouse embryonic fibroblasts (MEFs) were infected with *S. aureus* (supplementary material Fig. S2). By contrast, stable re-expression of human integrin β1 restored the accumulation of GM1 at the sites, where bacteria engaged the host integrin (supplementary material Fig. S2). These results demonstrate that fibronectin-binding *S. aureus* induces the redistribution of specific membrane microdomains upon contact with the host cell membrane.

Recruitment of membrane microdomains depends on the expression of staphyloccocal FnBP-A

To further corroborate the finding that integrin engagement by the bacteria is crucial to alter the distribution of membrane components, we infected integrin-expressing fibroblasts with either fibronectin-binding *S. aureus* strain MA12 or an isogenic mutant strain lacking both fibronectin-binding proteins (MA12 ΔFnBP-A/FnBP-B). After infection with Rhodamine-labeled bacteria for 2 hours, cells were fixed and GM1 was visualised using CT–FITC. Importantly, whereas cell contact of wild-type *S. aureus* MA12 again induced accumulation of GM1 in the vicinity of bacteria, the isogenic ΔFnBP-A/FnBP-B double mutant not only showed severely reduced adhesion to the host cells, but also completely lacked the ability to redistribute the ganglioside (supplementary material Fig. S3A). To confirm that membrane microdomain recruitment is triggered by staphylococcal FnBP, the commensal *Streptococcus gordonii* was transformed with the full-length FnBP-A sequence from *S. aureus*. Similarly to the non-pathogenic *Staphylococcus carnosus*, *S. gordonii* does not posses fibronectin-binding proteins and does not bind to fibronectin. However, the recombinant *S. gordonii* strain expressing staphylococcal FnBP-A (*S. gordonii* FnBP-A) was able to bind fibronectin (supplementary material Fig. S3B). Importantly, *S. gordonii* FnBP-A induced the local recruitment of GM1 upon host cell contact, whereas wild-type *S. gordonii* did not alter the distribution of GM1 (Fig. 2A). These data further demonstrate that FnBP-mediated contact to host integrin α5β1 is necessary to trigger the redistribution of plasma membrane components in the vicinity of cell-attached bacteria.

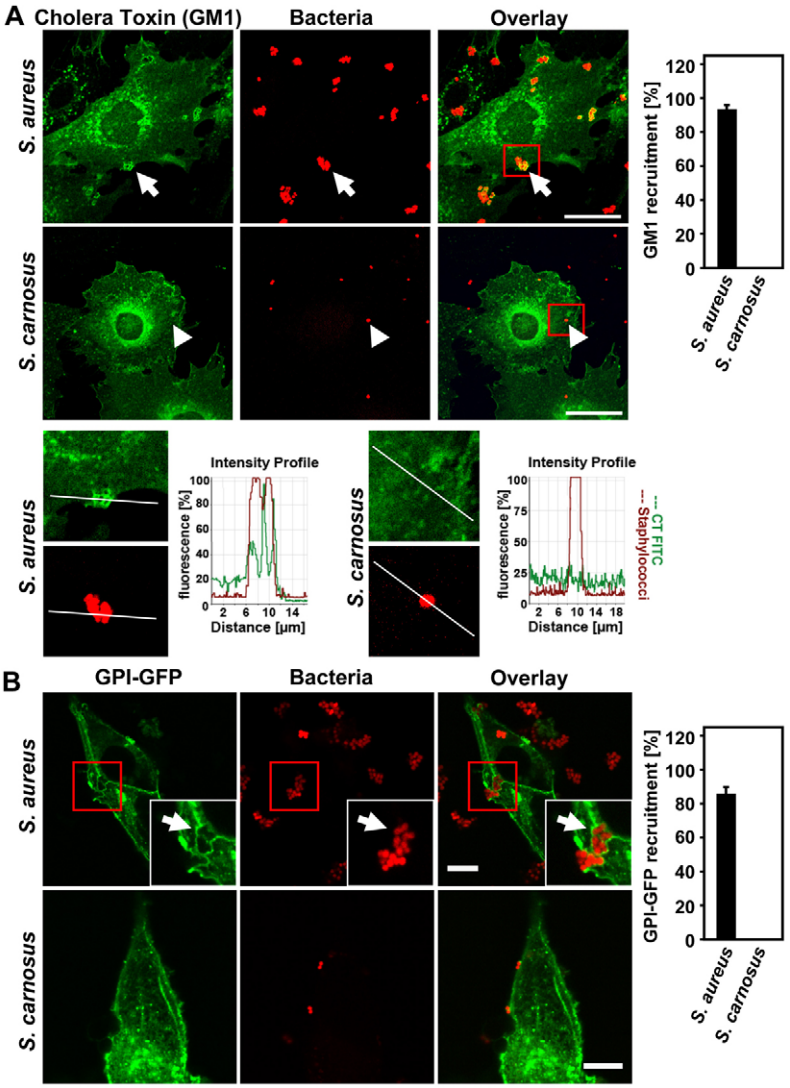

Fig. 1. Membrane microdomains accumulate in the vicinity of cell-attached *S. aureus*. (**A**) Integrin-expressing fibroblasts were infected for 2 hours with Rhodamine-labelled *S. aureus* Cowan or *S. carnosus*. After fixation, ganglioside GM1 was stained with CT–FITC. Samples were examined by confocal microscopy. Cell-associated *S. aureus* (arrows) or *S. carnosus* (arrowheads) are indicated. Scale bars: 10 µm. The marked areas (red box) were enlarged and the local recruitment of GM1-enriched membrane microdomains (green line) to cell-associated bacteria (red line) was quantified by plotting the fluorescence intensity as detected in the FITC and Rhodamine channels, respectively, against the distance. The percentage of GM1-recruiting bacteria was quantified by scoring all cell-associated bacteria for 20 cells each from three separate experiments. Bars represent the mean values ± s.d. (**B**) Fibroblasts were transfected with GFP–GPI and infected with Rhodamine-labelled *S. aureus* for 2 hours. The marked area is enlarged (red box) and shown as an inset. GFP–GPI recruitment to cell-associated *S. aureus* is indicated (arrows). Scale bars: 10 µm. The percentage of GPI–GFP-recruiting bacteria was quantified as in A.

S. aureus FnBP-A is sufficient to induce membrane microdomain recruitment

The results with wild-type and mutated *S. aureus* and *S. gordonii* strains do not rule out the possibility that upon first host cell contact via FnBP and fibronectin to integrin α5β1, additional bacterial products might be necessary to induce the recruitment of membrane microdomains. To investigate whether FnBP-initiated processes are sufficient to modulate the local composition of the plasma membrane, we used a recombinant, fibronectin-binding domain of *S. aureus* FnBP-A (GST-FnBP) (Agerer et al., 2003). Accordingly, polystyrene microbeads were covalently coupled with either GST–FnBP (FnBP beads) or GST alone (GST beads) and then incubated with human serum. Binding of plasma fibronectin to FnBP beads, but not to GST beads was detected after staining with a monoclonal anti-fibronectin antibody followed by flow cytometry analysis (Fig. 2B). The serum-treated beads were also incubated with integrin-expressing fibroblasts and the fixed samples were stained for GM1. Interestingly, FnBP-coupled beads strongly recruited the ganglioside GM1, whereas no recruitment was observed around GST-coupled beads (Fig. 2C). Furthermore, a GPI-anchored protein (GPI–GFP) also colocalized with ganglioside GM1 and FnBP-coupled beads (supplementary material Fig. S4). These results demonstrate that FnBP-mediated host cell contact is not only necessary, but also sufficient to recruit GM1-rich membrane microdomains.

Membrane microdomains have a functional role during the integrin-mediated uptake of *S. aureus*

Membrane microdomains are disrupted by cholesterol-chelating agents such as methyl-β-cyclodextrin (MβCD), nystatin or filipin. Therefore, human embryonic kidney (HEK293) cells were treated with increasing concentrations of MβCD 30 minutes before infection with *S. aureus* or *S. carnosus*, respectively. After 2 hours of infection, bacterial adhesion to the host cells and the amount of viable intracellular bacteria was determined. Importantly, attachment of *S. aureus* to the human cells was not disturbed by MβCD in the applied concentration range (Fig. 3A). However, MβCD treatment interfered in a dose-dependent manner with the uptake of *S. aureus* into host cells (Fig. 3B). Similar results were obtained with the cholesterol chelators filipin and nystatin, respectively (supplementary material Fig. S5). To further corroborate that the reduced number of viable intracellular bacteria is indeed due to a reduced integrin-mediated internalization, we measured cellular uptake of fluorescent bacteria by a flow cytometric assay (Pils et al., 2006). HEK293 cells were treated or not with MβCD and then infected with Fluorescein-labeled bacteria.

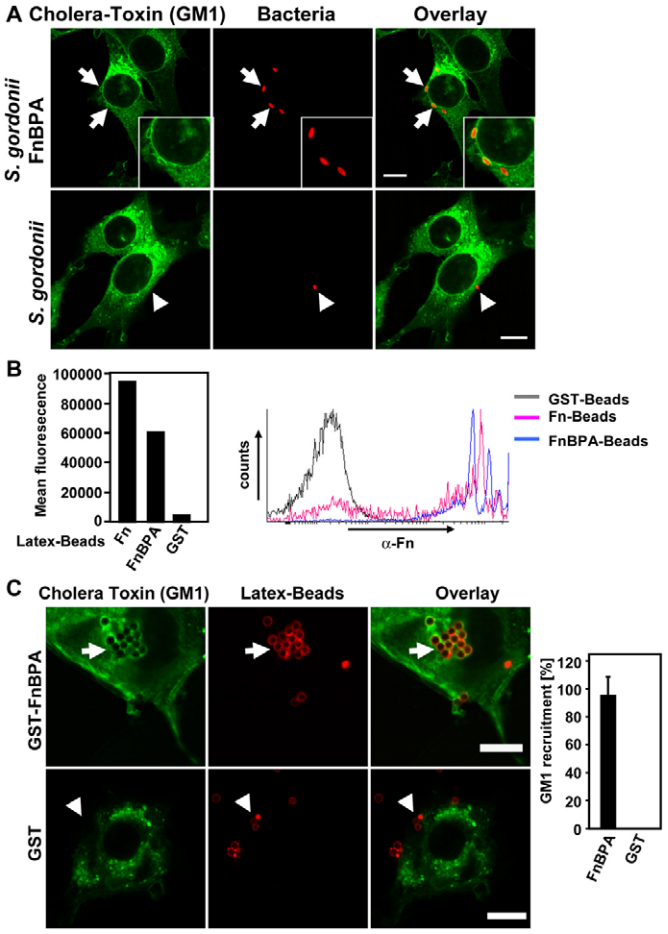

Fig. 2. Fibronectin-binding protein together with fibronectin is sufficient for the recruitment of GM1-enriched membrane microdomains. (**A**) Integrin-expressing fibroblasts were infected for 2 hours with FITC-labelled *S. gordonii* or *S. gordonii* expressing FnBP-A, respectively. After fixation, samples were stained with fluorescent cholera toxin B subunit. Cell-associated *S. gordonii* does not recruit GM1 (arrowhead), whereas FnBP-A-expressing *S. gordonii* recruits membrane microdomains (arrows). Scale bars: 10 µm. The inset shows an enlargement of the GM1 recruitment by *S. gordonii* FnBP-A. (**B**) FnBP-A B-domain-, fibronectin- and GST-coupled beads were incubated with human serum for 2 hours. After incubation, beads were washed and stained with monoclonal anti-fibronectin antibody (HFN7.1) followed by FITC-coupled goat-anti-mouse antibodies. Subsequently, beads were analyzed by flow cytometry. (**C**) Fibroblasts were incubated for 2 hours with FnBP-A B-domain-coupled beads or GST beads, respectively. After fixation, cells were stained for GM1. Beads coupled with FnBP-A (arrows), but not GST (arrowheads) recruit GM1. Scale bars: 10 µm. The percentage of GM1-recruiting microbeads was quantified by scoring all cell-associated beads for 20 cells each from three separate experiments. The bars represent the mean values ± s.d.

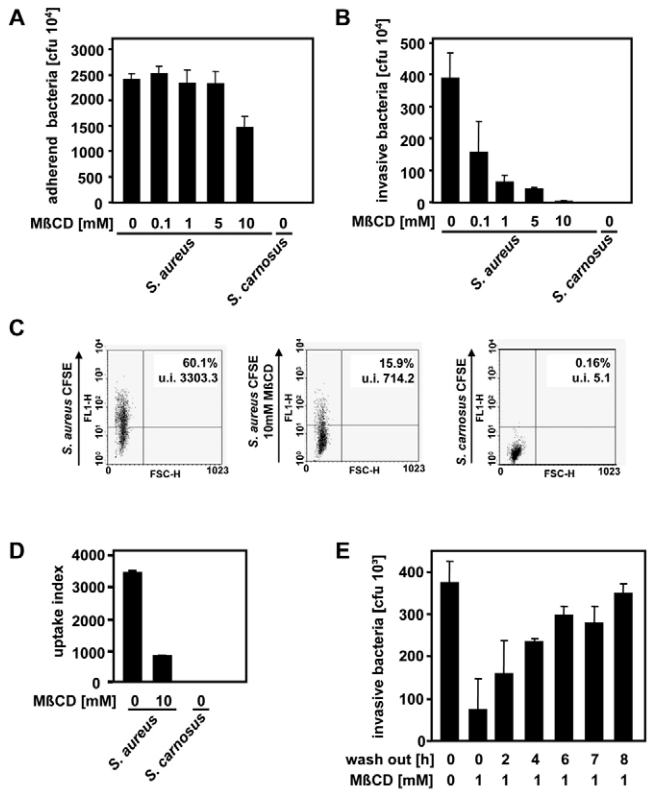

Fig. 3. Disruption of membrane microdomains impairs internalization of *S. aureus*. (**A**) Cells were treated with different concentrations of methyl-β-cyclodextrin (MβCD) and afterwards infected for 2 hours with *S. aureus* or *S. carnosus* at MOI 20. Cell-associated bacteria were quantified after detergent lysis of the eukaryotic cells and dilution plating of the bacteria on TSB plates. The graph shows mean values ± s.d. of a representative experiment done in triplicate. (**B**) Cells were treated as described in A, and intracellular bacteria were determined by gentamicin-lysostaphin protection assays. The bars represent mean values ± s.d. of a representative experiment done in triplicate. (**C**) HEK293 cells were infected with FITC-labelled *S. aureus* or *S. carnosus* for 2 hours. After washing, the fluorescence of extracellular bacteria was quenched by addition of Trypan Blue and the cell-associated fluorescence derived from intracellular bacteria was quantified by flow cytometry. Dot plots show a representative experiment, where the number indicates the percentage of cells harbouring intracellular bacteria. (FL1, intensity in the Fluorescein channel; FSC, forward scatter). (**D**) The number of internalized bacteria in C was estimated by multiplying the percentage of infected cells with the mean fluorescence intensity (uptake index). The bars represent mean values ± s.d. of a representative experiment done in triplicate. (**E**) HEK293 cells were treated or not with 1 mM MβCD. Cells were either infected for 2 hours immediately after the 30 minute MβCD treatment or after the indicated time following replacement of MβCD by regular growth medium (wash out). The number of intracellular bacteria was determined by gentamicin-lysostaphin protection assays. The bar graph shows mean values ± s.d. of an experiment done in triplicate.

Two hours after infection, the fluorescence of extracellular bacteria was quenched by addition of Trypan Blue and the remaining cell-associated fluorescence was taken as a direct measure for the amount of dead and viable intracellular bacteria. Accordingly, non-invasive bacteria, such as *S. carnosus*, do not lead to cell-associated fluorescence, whereas about 60% of the infected cell population contains intracellular *S. aureus* (Fig. 3C). Clearly, upon treatment with MβCD, uptake of *S. aureus* was strongly reduced compared with untreated cells (Fig. 3C,D).

To exclude the possibility of an overall cytotoxic effect of the cholesterol chelator, cells treated with 1 mM MβCD were infected for 2 hours with *S. aureus* either immediately after MβCD treatment or following different times of recovery in MβCD-free growth medium. Again, treatment with 1 mM MβCD strongly diminished internalization of the bacteria (Fig. 3E). However, this effect was reversible, and cells regained their ability to internalize *S. aureus* within 2–4 hours after withdrawal of MβCD (Fig. 3E). Eight hours after MβCD withdrawal, internalization of *S. aureus* by MβCD

pre-treated cells was comparable with untreated samples (Fig. 3E). These data indicate that ganglioside- and cholesterol-rich membrane microdomains have a crucial functional role during the integrin-β1-dependent uptake of *S. aureus* by mammalian cells.

Flotillin-1, flotillin-2 and caveolin, but not stomatin, are recruited to the site of infection

To determine whether membrane microdomain-associated proteins are involved in the internalization process of *S. aureus*, we analyzed the recruitment of stomatin, flotillin-1, flotillin-2 and caveolin. These proteins are known to localize to cellular membranes, including the plasma membrane and all are enriched in membrane microdomains (Browman et al., 2007; Frick et al., 2007; Neumann-Giesen et al., 2004; Salzer and Prohaska, 2001). MEFs were transfected with constructs encoding the indicated GFP-tagged proteins, infected with fluorescence labeled *S. aureus* and stained with Alexa-Fluor-555-coupled cholera toxin b subunit (CT-555). In the case of stomatin, no colocalization between this protein, *S. aureus* and GM1 was detected (Fig. 4). By contrast, both flotillin-1 and flotillin-2 were strongly recruited to cell-attached *S. aureus* together with ganglioside GM1 (Fig. 4). Furthermore, limited recruitment of GFP–caveolin was observed (Fig. 4), which was most pronounced within 30 minutes after *S. aureus* contact with host cells.

Caveolin-1 deficiency enhances integrin-mediated uptake of *S. aureus*

To test the functional significance of the membrane microdomain organizing proteins for bacterial internalization, we first overexpressed dominant-negative forms of flotillin-1 or flotillin-2 that were reported to interfere with flotillin-enriched raft formation (Neumann-Giesen et al., 2004). Importantly, no alteration of *S. aureus* invasion could be observed in the presence of these flotillin mutants, suggesting that flotillins have no functional relevance in this process (supplementary material Fig. S6). To investigate the role of caveolin, we used a fibroblast line derived from caveolin-1-deficient mice (*Cav1*$^{-/-}$ cells) (Drab et al., 2001). Surprisingly, uptake of *S. aureus* by *Cav1*$^{-/-}$ cells was strongly enhanced compared with that in wild-type fibroblasts (CavWT), whereas bacterial attachment to the cell surface was indistinguishable between the two cell types (Fig. 5A,B). These observations suggested that the presence of caveolin-1 does not alter the availability of integrin α5β1 on the cell surface, but interferes with endocytosis of fibronectin-coated bacteria. We also verified the complete lack of caveolin-1 expression in *Cav1*$^{-/-}$ cells by western blot analysis and analyzed the expression of integrin β1, α-actinin and vinculin, respectively. Expression of integrin β1 and associated proteins was not altered in *Cav1*$^{-/-}$ cells compared with CavWT cells (Fig. 5C). Scanning electron microscopy (SEM) suggested that FnBP-coated microbeads were more efficiently internalized by *Cav1*$^{-/-}$ cells compared with wild-type cells, and *Cav1*$^{-/-}$ cells were often observed to take up large clusters of particles (Fig. 5D). The uptake of bacteria in *Cav1*$^{-/-}$ cells was still sensitive to MβCD treatment, indicating that the enhanced internalization in these cells does not occur by a mechanistically distinct endocytic pathway (supplementary material Fig. S7).

To analyze whether the inhibitory capacity of caveolin is a general phenomenon, we tested an additional example of integrin-mediated bacterial uptake. Therefore, we used isogenic *Neisseria gonorrhoeae* strains, which either express a fibronectin-binding adhesin (Ngo Opa_{50}) or do not express any Opa protein (Ngo Opa^{-}). Similarly to the FnBP adhesin of *S. aureus*, the Opa_{50} protein of *N. gonorrhoeae* engages integrin α5β1 indirectly via recruitment of fibronectin (van Putten et al., 1998). Importantly, a comparable increase in internalization was observed when *Cav1*$^{-/-}$ cells were infected with the Opa_{50}-expressing strain in the presence of fibronectin, whereas the non-opaque bacteria were hardly internalized by both cell lines (Fig. 5E). These results demonstrate that caveolin diminishes uptake of fibronectin-coated microbes via integrin α5β1 and suggest that the inhibitory function of caveolin might pertain to the integrin-mediated uptake of ligand-coated particles in general.

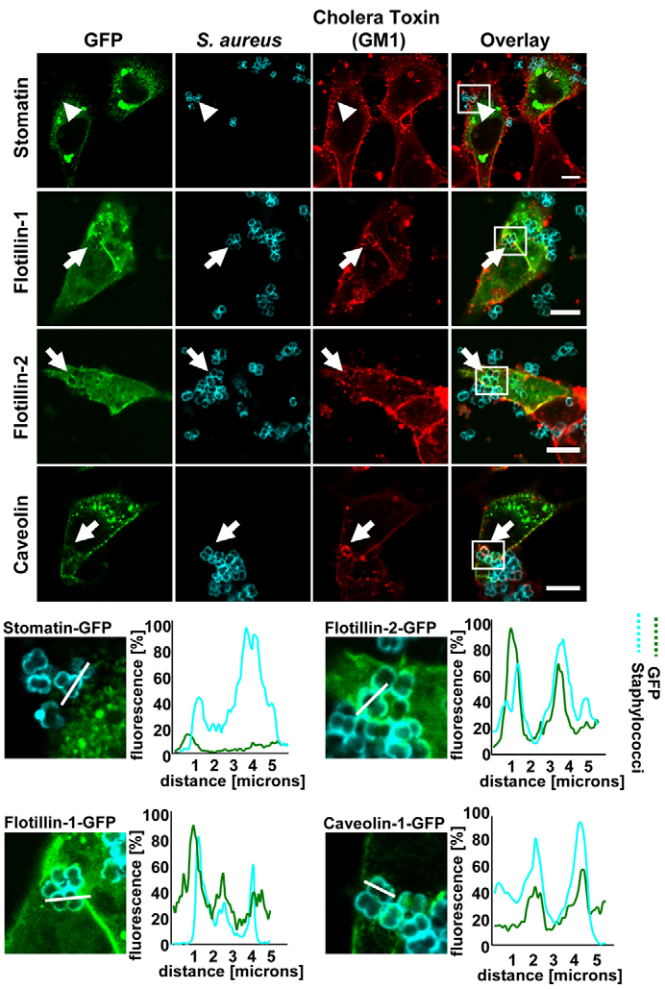

Fig. 4. A distinct set of membrane-microdomain-associated proteins is recruited to the site of staphylococcal attachment. Integrin-expressing fibroblasts were transfected with constructs encoding the GFP-tagged membrane microdomain marker proteins stomatin, flotillin-1, flotillin-2 and caveolin-1. Cells were infected for 2 hours with biotin-labelled *S. aureus*. After fixation and permeabilization, ganglioside GM1 was stained with cholera toxin and the bacteria were visualized with streptavidin–Cy5. Recruitment of fluorescent proteins to GM1 and cell-attached bacteria is indicated by white arrows. The arrowhead indicates the lack of stomatin recruitment to cell-associated bacteria. Scale bars: 10 µm. The marked areas (white boxes) were enlarged and the local recruitment of GFP or the GFP-tagged proteins (green line) to cell-associated bacteria (cyan line) was quantified by plotting the fluorescence intensity as detected in the FITC and Cy5 channels, respectively, along the indicated white line against the distance.

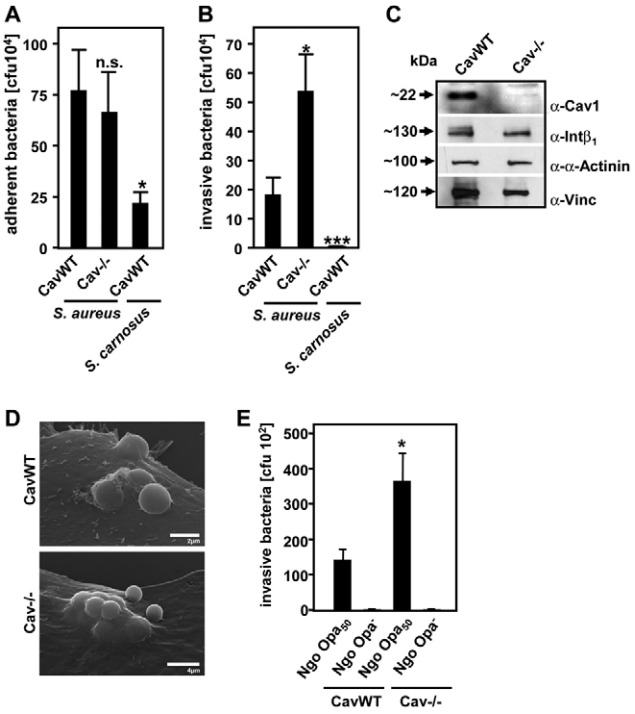

Fig. 5. The presence of caveolin negatively regulates bacterial internalization. (**A**) Wild-type (CavWT) or caveolin-1-deficient (*Cav1*$^{-/-}$) mouse fibroblasts were infected for 2 hours with *S. aureus* or *S. carnosus*. Total cell-associated bacteria were quantified. The bars show mean values ± s.e.m. of three independent experiments done in triplicate. Samples were compared with CavWT cells infected with *S. aureus* and significance was evaluated by Mann-Whitney Test. **P*<0.05; n.s. not significant. (**B**) Cells were infected as in A and intracellular bacteria were determined by gentamicin-lysostaphin protection assays. Data were evaluated as in A. **P*<0.05; ****P*<0.001. (**C**) Caveolin expression in CavWT and *Cav1*$^{-/-}$ cells was evaluated by western blotting of whole-cell lysates with monoclonal anti-caveolin-1 antibody. Expression of integrin β_1, α-actinin and vinculin was also analyzed. (D) CavWT and *Cav1*$^{-/-}$ cells were incubated with FnBP-coated microbeads for 2 hours. Samples were fixed and analyzed by scanning electron microscopy (SEM). (**E**) CavWT and *Cav1*$^{-/-}$ cells were infected with *N. gonorrhoeae* Opa_{50} or *N. gonorrhoeae* Opa^- for 2 hours at MOI 100 in the presence of fibronectin. Internalization of bacteria was measured by gentamicin protection assay. The graph shows mean values ± s.e.m. of two independent experiments done in triplicate. Statistical significance was evaluated by Mann-Whitney Test. **P*<0.05.

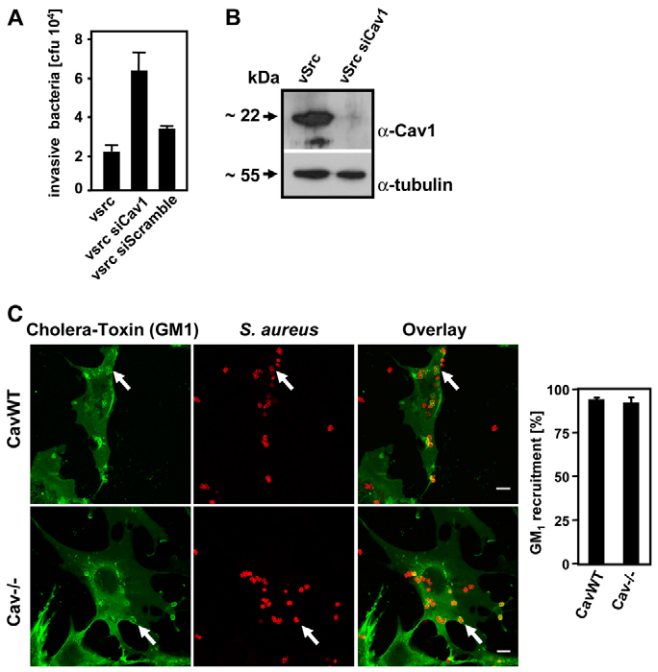

Fig. 6. Enhanced bacterial uptake in *Cav1*$^{-/-}$ cells is independent of modulation of Src activity or increased membrane microdomain recruitment. (**A**) NIH v-Src cells were treated with siRNA against caveolin for 48 hours before infection with *S. aureus* for 2 hours. Intracellular bacteria were determined by gentamicin-lysostaphin protection assay. The bars represent mean values ± s.e.m. of a representative experiment done in triplicate. (**B**) Caveolin expression in NIH v-Src cells, treated with siRNA against caveolin, was evaluated by western blotting of whole-cell lysates with anti-caveolin-1 antibody (upper panel). The membrane was stripped and re-probed with antibodies against α-tubulin (lower panel). (**C**) CavWT and *Cav1*$^{-/-}$ cells were infected with Rhodamine-labeled *S. aureus* for 2 hours. After infection, cells were fixed and stained with CT-FITC without prior permeabilization to selectively detect surface localized GM1. Recruitment of GM1-enriched membrane microdomains to cell-attached bacteria is indicated by arrows. Scale bars: 10 µm. The percentage of GM1-recruiting bacteria was quantified by scoring all cell-associated bacteria of 15 cells each from three separate experiments. The bars represent the mean values ± s.d.

Enhanced bacterial uptake by *Cav1*$^{-/-}$ cells is not due to modulation of Src activity or increased recruitment of membrane microdomains

Caveolin is a substrate of Src family protein tyrosine kinases (PTKs) and has been suggested to act in a negative-feedback loop to limit Src PTK activity via the recruitment of C-terminal Src kinase (CSK) (Neet and Hunter, 1995). As the integrin-mediated uptake of *S. aureus* requires Src PTC activity (Agerer et al., 2003), we wondered whether the inhibitory effect of caveolin-1 on integrin-mediated internalization might be due to Csk inhibition of Src PTCs. Therefore, we used fibroblasts expressing a constitutively active, truncated form of Src (v-Src) that cannot be regulated by CSK. Importantly, siRNA-mediated knockdown of caveolin-1 increased the integrin-mediated internalization of *S. aureus* by NIH v-Src cells to a similar extent as observed before with wild-type fibroblasts (Fig. 6A). These results suggested that increased uptake of bacteria in *Cav1*$^{-/-}$ cells is not due to the release of a caveolin-dependent inhibitory feedback loop impinging on Src activity. Therefore, caveolin-1 blocks integrin-mediated endocytosis of *S. aureus* by a mechanism distinct from its effect on Src activity.

A further explanation for the surprising inhibitory role of caveolin-1 during integrin-mediated uptake of *S. aureus* could be that a lack of caveolin-1 releases limiting membrane microdomain components from caveolae, leading to enhanced accumulation of GM1-enriched membrane microdomains at the site of pathogen-host cell contact. However, microscopic analysis of GM1 distribution at the cell surface revealed a similar extent of GM1-positive membrane microdomains surrounding fibronectin-bound bacteria in both *Cav1*$^{-/-}$ and CavWT cells (Fig. 6B). This is in line with previous reports that have found similar amounts of GM1 at the surface of adherent caveolin-1-expressing and caveolin-1-deficient cells (del Pozo et al., 2005). Therefore, caveolin-1 does not seem to sequester membrane components to interfere with membrane microdomain-mediated uptake.

Caveolin-1 interferes with membrane protein mobility and blocks integrin-mediated uptake of *S. aureus*

Caveolin-1 has oligomerization and scaffolding functions that stabilize the lipid microenvironment in the membrane, and this capacity might interfere with membrane mobility required for bacterial internalization. Therefore we used fluorescence recovery after photobleaching (FRAP) experiments to determine the degree of mobility of a membrane-microdomain-associated protein in the presence or absence of caveolin. CavWT and *Cav1*$^{-/-}$ cells were transfected with GFP–GPI as a marker for membrane microdomains. After bleaching a defined region of interest (ROI), the half-life times of fluorescence recovery were measured and the diffusion coefficient was calculated. Clearly, mobility of GFP–GPI was increased in *Cav1*$^{-/-}$ cells compared with CavWT cells (Fig. 7A). We further performed FRAP experiments with GFP–GPI-transfected cells upon infection with *S. aureus*. Mobility of GFP–GPI was also strongly increased in the membrane microdomains surrounding the integrin-bound bacteria in cells lacking caveolin compared with CavWT cells (Fig. 7B). Importantly, mobility of CEACAM3, a receptor that does not localize to membrane microdomains (Muenzner et al., 2008; Schmitter et al., 2007), is not altered in *Cav1*$^{-/-}$ cells (Fig. 7C), whereas mobility of GM1, as a second independent marker of membrane microdomains, is also increased in *Cav1*$^{-/-}$ cells (supplementary material Fig. S8). These results suggest that caveolin-1 selectively suppresses the mobility of membrane microdomain components.

To investigate whether alterations in the mobility of membrane microdomain components could be mechanistically linked to integrin-mediated uptake of bacteria, we treated cells with Tween20, a detergent that has been shown to enhance the mobility of membrane proteins (Ghosh et al., 2002; Sergent et al., 2005). Tween20 did not affect bacterial adhesion, but strongly increased the number of internalized bacteria (Fig. 7D). Similarly to chemical agents, physical parameters such as temperature have a strong effect on the fluidity of membrane lipids and the mobility of membrane proteins. Thus, we transfected MEFs with GFP–GPI and monitored the mobility of membrane microdomains at 33°C, 37°C and 41°C. Mobility of GFP–GPI was strictly correlated with temperature (Fig. 7E). Accordingly, the diffusion coefficient *D* for GFP–GPI was highest at 41°C, and at this temperature, the *D* value for GFP–GPI in wild-type fibroblasts was comparable with that observed in *Cav1*$^{-/-}$ cells at 37°C (Fig. 7E). Infection of fibroblasts under the different temperature regimes revealed that enhanced membrane mobility at 41°C correlated with increased bacterial uptake, whereas decreased membrane mobility at 33°C was associated with decreased bacterial internalization (Fig. 7E). Together, these data indicate membrane microdomain mobility, which can be modulated by caveolin-1, as a limiting factor for integrin-mediated bacterial internalization.

Caveolin scaffolding function is required for reduced mobility of membrane-microdomain-associated proteins

Mutations in caveolin-3 in the N-terminal oligomerization and scaffolding domain have been described in muscle dystrophy patients (McNally et al., 1998). In contrast to several other point mutations or microdeletions in this part of caveolin-3, the missense mutation G55S in caveolin-3 does not interfere with the normal transport of the protein to the plasma membrane, but affects membrane protein trafficking (Hernandez-Deviez et al., 2008). Therefore, we introduced the corresponding mutation into the scaffolding domain of caveolin-1 (G83S) by site-directed mutagenesis (Fig. 8A). Upon expression of wild-type caveolin-1 in *Cav1*$^{-/-}$ cells, uptake of FnBP-coated latex beads was severely reduced compared with *Cav1*$^{-/-}$ cells transfected with a cerulean-

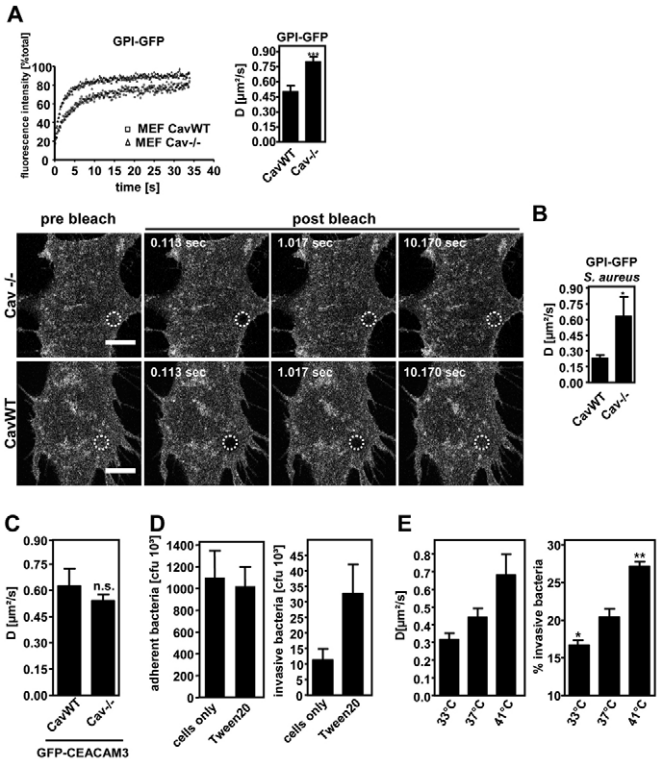

Fig. 7. Mobility of membrane microdomains positively correlates with integrin-mediated internalization of *S. aureus*. (**A**) CavWT and *Cav1*$^{-/-}$ cells were transfected with GFP–GPI. A region of interest (ROI) was bleached with high laser intensity. Recovery of fluorescence was recorded every 0.113 seconds after bleaching. Representative FRAP curves are shown for CavWT and *Cav1*$^{-/-}$ cells, respectively. From half-life times of fluorescence recovery the diffusion coefficient D was calculated from FRAP measurements in 14 cells, each. Statistical significance was evaluated by unpaired *t*-test. ***P<0.001. Representative images from one FRAP experiment, including one pre-bleach and three post-bleach images from the indicated time points, are shown. Images at 0.113 second represent the first image after bleaching. Bleaching area is indicated as a punctate circle. Scale bars: 10 µm. (**B**) CavWT and *Cav1*$^{-/-}$ cells were transfected with GFP–GPI. The next day cells were infected with Rhodamine-labelled *S. aureus* for 1 hour and analyzed by FRAP. A small region of recruited GFP–GPI close to the bacteria was bleached. FRAP was performed and evaluated as described in A. *P<0.05. Scale bars: 10 µm. (**C**) CavWT and *Cav1*$^{-/-}$ cells were transfected with GFP–CEACAM3 and analyzed by FRAP as in A. The diffusion coefficient D was calculated from FRAP measurements in ten cells, each. Statistical significance was evaluated by unpaired *t*-test. n.s., not significant, P>0.05. (**D**) Integrin-expressing fibroblasts were treated with Tween20 for 30 minutes. Treated cells were infected with *S. aureus* for 2 hours at MOI 20. Total cell-associated (left panel) and intracellular bacteria (right panel) were determined. The bars represent mean values ± s.e.m. of two experiments done in triplicate. (**E**) Integrin-expressing fibroblasts were transfected with GFP–GPI. FRAP experiments were performed at 33°C, 37°C, and 41°C and evaluated as described in A. Diffusion coefficient *D* was calculated from FRAP measurements in 14 cells each (left panel). Parallel samples were infected with *S. aureus* for 2 hours at MOI 20. After infection, total cell-associated and intracellular bacteria were determined in parallel samples. The bar represents mean percentage of invasive bacteria ± s.e.m. of two experiments done in triplicate. Statistical significance was evaluated by Mann-Whitney Test. *P<0.05; **P<0.01.

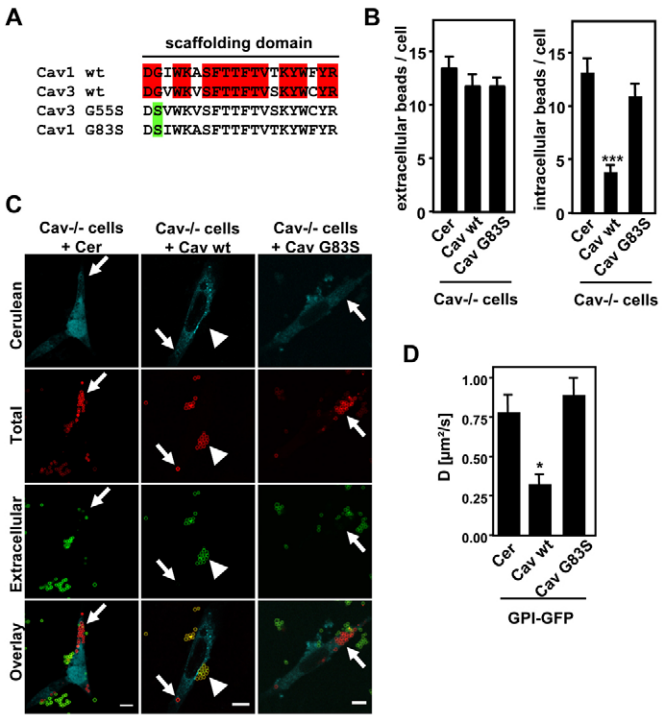

Fig. 8. Caveolin-1 wild type, but not a scaffolding domain mutant, suppresses membrane microdomain mobility and FnBP-triggered uptake. (**A**) Amino acid alignment of the human caveolin-1 and caveolin-3 scaffolding domain. Identical amino acids are highlighted in red and the G55S mutation in caveolin-3 as well as the analogous G83S point mutations in caveolin-1 are indicated in green. (**B**) *Cav1*$^{-/-}$ cells were transfected with a cerulean (Cer)-encoding control vector or plasmids coding for wild-type caveolin-1–cerulean (Cav wt) or G83S caveolin-1–cerulean (Cav G83S) and incubated with biotin- and Rhodamine-labelled FnBP-coated beads for 2 hours. After fixation, extracellular beads were stained with streptavidin–Cy2. Number of intra- and extracellular beads per cells from each sample was determined from 40 cells of two independent experiments. Statistical significance was evaluated by Mann-Whitney Test. ***P<0.001. (**C**) Samples from B were analyzed by confocal microscopy. Arrows indicate intracellular bacteria (red in the overlay), whereas arrowheads highlight extracellular bacteria (yellow in the overlay). Scale bars: 10 µm. (**D**) *Cav1*$^{-/-}$ cells were transfected with GFP–GPI together with a cerulean (Cer)-encoding control vector or plasmids encoding Cav wt or Cav G83S, respectively. FRAP experiments were performed and the diffusion coefficient D for GFP–GPI was calculated from FRAP measurements in ten cells, each. Statistical significance was evaluated by unpaired *t*-test. *P<0.05; n.s., not significant.

encoding control construct, further confirming the inhibitory role of this membrane-microdomain-associated protein (Fig. 8B,C). By contrast, re-expression of caveolin-1 G83S did not affect the efficient internalization of FnBP-coated latex beads (Fig. 8B,C). Importantly, the G83S mutation in the scaffolding domain also abolished the ability of caveolin-1 to suppress membrane mobility of GFP–GPI (Fig. 8D), strongly supporting the idea that caveolin-1 affects uptake of integrin-associated bacteria by interfering with the mobility of membrane microdomain components via its scaffolding function.

Discussion

Numerous bacterial pathogens and viruses not only bind to integrins on the surface of host cells, but also exploit the endocytotic properties of these receptors to get access to an intracellular niche. We show here that the internalization of fibronectin-coated bacteria requires the integrin-initiated recruitment of sphingolipid- and cholesterol-rich membrane microdomains. The uptake process seems to depend on the mobility of membrane microdomain components and is modulated by the presence of the protein caveolin-1, the ambient temperature or agents that change membrane mobility. These data highlight the close functional link between integrin engagement and the spatial organization of the plasma membrane, but also imply a role for caveolin-1-mediated scaffolding of membrane microdomain components to suppress their endocytosis.

Cell entry by several different pathogens that engage distinct surface receptors involves membrane microdomains (Gulbins et al., 2004; Lafont and van der Goot, 2005; Riethmuller et al., 2006). Depletion of cholesterol or a lack of membrane sphingolipids impairs entry of *Shigella flexneri* (Lafont et al., 2002). Because cholesterol depletion affects the interaction between the *Shigella* effector protein IpaB and its cellular receptor CD44, the integrity of lipid rafts is crucial for the initial host cell contact in this context (Lafont et al., 2002). In the case of *Listeria monocytogenes*, it has been demonstrated that cell contact of the bacteria via distinct adhesive proteins, the E-cadherin-binding Internalin A (InlA) as well as the c-Met-binding InlB, results in the recruitment of membrane microdomain components such as ganglioside GM1 as well as GPI-linked proteins (Seveau et al., 2004). Depletion of cholesterol before infection with InlA-expressing *Listeria* or before incubation with InlA-coated microbeads reduces clustering of E-cadherin and affects the initial adhesion to the eukaryotic cells (Seveau et al., 2004).

This is different from the situation we observed for *S. aureus* FnBP-mediated host-cell contact, where cholesterol depletion selectively affects the endocytosis, but not the adhesion of the bacteria to the receptor. An analogous observation has been made for *S. pyogenes* strains that connect to host cell integrin α5β1 via fibronectin, which is similar to staphylococci in this respect (Talay et al., 2000). Methyl-β-cyclodextrin treatment blocks internalization of *S. pyogenes*, but not host cell association (Rohde et al., 2003). Similarly, outer-membrane vesicles of *Porphyromonas gingivalis*, which cluster integrin β1 upon host cell contact, exhibit diminished internalization by cholesterol-depleted or sphingolipid-deficient cells, whereas host cell adhesion of *P. gingivalis* membrane vesicles is not compromised under these conditions (Tsuda et al., 2008). Furthermore, host cell adhesion by *Salmonella typhimurium* is undisturbed by methyl-β-cyclodextrin treatment, even though cholesterol-rich membrane domains are crucial during *Salmonella* invasion (Garner et al., 2002). These results suggest that availability and clustering of some receptors, such as integrin β1, on the surface of eukaryotic cells is not dependent on membrane microdomains, whereas other surface receptors such as E-cadherin or CD44 might allow functional interactions only in the presence of intact cholesterol- and sphingolipid-rich membrane microdomains. That membrane microdomain organization is downstream of integrin activation and not a prerequisite for integrin engagement is also supported by studies reported by Gaus and colleagues (Gaus et al., 2006). Upon release of cells from the substrate, the organization of GM1-containing membrane regions is strongly perturbed, whereas in adherent cells, where high-affinity, active integrins are engaged by a physiological ligand, membrane order is re-established (Gaus et al., 2006).

A clear mechanistic difference in membrane-microdomain-mediated uptake of different bacteria relates to the role of caveolin-

1. Whereas siRNA-mediated knockdown of caveolin-1 expression results in a reduction of InlA-triggered uptake of *Listeria* (Bonazzi et al., 2008), caveolin-1 deficiency leads to increased internalization of *S. aureus*. This discrepancy might be connected to the above-mentioned difference in the dependence on membrane microdomains for clustering of the involved receptors, for either E-cadherin or integrin β1, respectively. Indeed, caveolin-1 knockdown impairs recruitment of E-cadherin to the sites of bacterial attachment, thereby contributing to reduced E-cadherin-mediated uptake of InlA-expressing bacteria (Bonazzi et al., 2008).

In support of our findings, several investigations have indicated a negative regulatory role of caveolin for endocytotic processes. SV40, a non-enveloped DNA virus, uses the endocytotic properties of caveolae to enter cells and to reach the endoplasmic reticulum (Pelkmans et al., 2001). Interestingly, caveolin-1-deficient murine fibroblasts internalize SV40 more efficiently than caveolin-1-expressing cells (Damm et al., 2005). Similar conclusions have been reached by studying physiological endocytotic processes, including internalization of autocrine motility factor receptor, endocytosis of dysferlin, a membrane protein of skeletal muscle cells, or internalization of GM1-containing membrane microdomains (Hernandez-Deviez et al., 2008; Lajoie et al., 2009b; Le et al., 2002). In all three cases, the presence of caveolin-1 correlates with reduced endocytosis of the studied molecules. These results, together with our findings, suggest that caveolin-1 impairs rather than promotes uptake of particular cholesterol- and sphingolipid-rich membrane microdomains and associated components (Kirkham and Parton, 2005).

Caveolin-1 has also been reported to be crucial for the transport of GPI-linked proteins from the Golgi complex to the plasma membrane (Sotgia et al., 2002). However, the caveolin-1-deficient cells isolated from mice generated by Kurzchalia and colleagues (Drab et al., 2001) that were used in our study do not show an alteration in the surface transport and surface localization of GPI-anchored proteins compared with wild-type fibroblasts (Manninen et al., 2005). Clearly, caveolin-1 functions as a protein scaffold and participates in the distribution of membrane components into spatially separated subdomains (Lajoie et al., 2009a). An analogous membrane-organizing function is mediated by proteins of the SPFH domain family, which encompasses flotillin-1 and flotillin-2, as well as stomatin (Browman et al., 2007). Similarly to caveolin, the SPFH-domain-containing proteins oligomerize to create stable membrane platforms (Sargiacomo et al., 1995; Solis et al., 2007). However, although flotillins are abundant in membrane microdomains surrounding cell-attached *S. aureus*, they do not appear to influence internalization of these bacteria. Therefore, obstruction of integrin-mediated particle uptake is not a general feature of oligomeric, membrane-microdomain-associated proteins.

Overlapping with the oligomerization domain, caveolins possess a scaffolding domain (caveolin scaffolding domain, CSD), which associates with membrane proteins containing a complete or partial ΦxΦxxxxΦxxΦ motif, where Φ represents an aromatic amino acid (Couet et al., 1997). Interestingly, the integrin α5 subunit contains a ΦxxΦxxxΦΦ sequence at the interface of the transmembrane and the cytosolic domain, which is reminiscent of the CSD binding motif. Indeed, a link between caveolin-1 and several integrin α-subunits has been reported previously (Wary et al., 1998). Supporting the idea that the scaffolding properties of caveolin are important to limit the mobility of membrane microdomain components and to suppress the endocytosis of integrin-bound bacteria, a point mutation in the CSD abolished the ability of caveolin-1 to modulate these cellular functions. It is important to note that the analogous point mutation in the caveolin-3 CSD is associated with muscular dystrophy and affects the internalization of the muscle-specific membrane protein dysferlin (Hernandez-Deviez et al., 2008; McNally et al., 1998). Accordingly, scaffolding of surface proteins in cholesterol- and sphingolipid-rich membrane domains by caveolins might be a common means to prevent or slow down endocytosis of distinct receptors. From a conceptual point of view, it is highly plausible that in contrast to many signaling receptors, which are rapidly endocytosed upon ligand binding, receptors with adhesive functions should be stabilized at the plasma membrane upon binding of their ligand.

Together, our data suggest that integrin engagement by fibronectin-coated bacteria induces the formation of a cholesterol- and sphingolipid-rich membrane microenvironment. The transient recruitment of caveolin-1 and the scaffolding function of this oligomeric protein interfere with the mobility of membrane microdomain components and stabilize the ligand-occupied integrin at the plasma membrane. Accordingly, caveolin-1 is able to curtail the internalization of ECM-coated bacteria as we report here. Interestingly, genetic deletion of caveolin-1, mild detergents or enhanced ambient temperature promote membrane mobility and at the same time, these treatments enhance the uptake of *S. aureus* via fibronectin-binding integrin α5β1. Modulation of membrane mobility by cellular factors and by systemic responses, such as fever, is a novel aspect of pathogen–host interaction that could represent a decisive factor during invasion by obligatory and facultative intracellular bacterial pathogens. More importantly, the impairment of membrane microdomain mobility mediated by the caveolin-1 scaffolding domain might have an important role in regulating the endocytosis of distinct surface receptors, thereby affecting numerous physiological processes.

Materials and Methods

Reagents and antibodies

Cytochalasin D and nystatin were obtained from Calbiochem (Bad Soden, Germany), methyl-β-cyclodextrin and filipin from Sigma (Schnelldorf, Germany), Tween20 from Applichem (Darmstadt, Germany). Bovine fibronectin was from ICN Biomedicals (Eschwege, Germany), NHS-LC-Biotin from Perbio Science (Rockford, IL). Monoclonal antibodies against human fibronectin (clone IST-4), against α-actinin (clone BM-75.2) and against vinculin (clone hVin-1) were from Sigma, against GFP (clone JL-8) from Clontech (Saint-Germain-en-Laye, France), against caveolin-1 (clone 2297) from BD Transduction Laboratories (Heidelberg, Germany). Monoclonal antibodies against human fibronectin (clone HFN7.1), against tubulin (clone E7), and against integrin β1 (clone AIIB2) were purified from hybridoma supernatants (DSHB, University of Iowa, IA). Secondary antibodies and streptavidin–Cy5 were from Jackson ImmunoResearch (West Grove, PA). Cholera toxin subunit B–Alexa Fluor 555 (CT-555) was obtained from Invitrogen (Karlsruhe, Germany) and CT–FITC was from Sigma. Shiga toxin was provided by Ludger Johannes (Institute Curie, Paris, France). 5-(6)-carboxyfluorescein-succinylester and the corresponding tetramethylrhodamine-dye were purchased from Molecular Probes (Eugene, OR).

Bacteria

S. aureus Cowan and non-pathogenic *S. carnosus* TM300 were described previously (Agerer et al., 2003). The ΔFnBP-A/FnBP-B mutant in *S. aureus* strain MA12 was constructed by transduction of the *fnbA::tet* and *fnbB::ermB* mutation from strain 8325-4 (Greene et al., 1995) to MA12 using phage Φ85. Staphylococci were cultured in Tryptic Soybean Broth (TSB; BD Biosciences, Heidelberg, Germany) at 37°C and harvested in mid-logarithmic phase. FnBP-A protein was heterologously expressed on the surface of *S. gordonii* GP1221 using the host integration system as described (Oggioni and Pozzi, 1996). The *fnbA* gene was amplified via PCR using forward primer: 5′-AAA GAA GCT GCA GGA TCC GAA CAA AAG AC-3′ and reverse primer: 5′-GGG TCG ACT TTA GAA GGC TTT TTA GGT TCT T-3′. The gene was cloned into plasmid vector pSMB103 to give functional in-frame fusion with the signal sequence and the membrane anchor coding regions of the *emm6* gene, and inserted via gene replacement as a gene cassette into a defined chromosomal locus of the *S. gordonii* chromosome, resulting in surface expression of a functional FnBP-A protein. Streptococci were cultured in TSB in static culture at 37°C. Before

infection, bacteria were washed once in sterile PBS and adjusted to 1×10^8 c.f.u./ml in PBS. In some experiments, staphylococci were fluorescently labelled before infection as described (Agerer et al., 2003; Agerer et al., 2004). *Neisseria gonorrhoeae* strain MS11 N303 (expressing the fibronectin-binding Opa_{50}) and the isogenic non-opaque strain MS11 N302 (Kupsch et al., 1993) were provided by Thomas F. Meyer (MPI for Infection Biology, Berlin, Germany) and cultured on GC-agar plates at 37°C and 5% CO_2. For infection experiments, bacteria were grown to exponential growth phase in HEPES buffer enriched with proteose peptone as described (van Putten et al., 1998) at 37°C for 2 hours.

Cell culture

HEK293 cells were grown in DMEM with 10% calf serum (CS) at 37°C in 5% CO_2. Mouse embryonic fibroblasts (MEFs) derived from caveolin-1-knock-out mouse embryos (*Cav1*$^{-/-}$ cells) originally generated by Drab and colleagues (Drab et al., 2001) as well as caveolin wild-type cells (CavWT) were obtained from Ari Helenius (ETH Zürich, Switzerland). MEFs from integrin-β1-knockout mouse embryos (*Int*$^{-/-}$ cells) and human integrin-β1 re-expressing *Int*$^{-/-}$ cells (integrin-expressing fibroblasts) were provided by Reinhard Fässler (MPI for Biochemistry, Martinsried, Germany). MEFs were cultured in DMEM with 10% fetal calf serum (FCS) supplemented with non-essential amino acids and pyruvate on gelatine-coated (0.1% gelatine in PBS) cell culture dishes. NIH v-Src cells were cultured as described (Hauck et al., 2002). All cell lines were subcultured every 2–3 days and were regularly checked for the absence of mycoplasma.

Recombinant DNA constructs and transfection of cells

Expression constructs encoding GL-GPI–GFP, caveolin-1–GFP and stomatin–GFP were kindly provided by Lucas Pelkmans (ETH Zürich, Switzerland), caveolin-1–Myc–mRFP was provided by Ivan Nabi (Life Science Institute, Vancouver, Canada), flotillin-2 7xYF–GFP, flotillin-2-G2A–GFP and flotillin-2–GFP were provided by Ritva Tikkanen (University Clinic of Frankfurt am Main, Germany), flotillin-2-EA–GFP was obtained from Claudia A. O. Stürmer (University of Konstanz, Konstanz, Germany) and flotillin-1-GFP was provided by Benjamin J. Nichols (MRC Laboratory of Molecular Biology, Cambridge, UK). The caveolin-1–Cerulean construct was generated by PCR amplification using caveolin-1–Myc–mRFP as template and primers hCaveolin-sense 5′-GAAGTTATCAGTCGACACCATGTCTGGGGGCA-AATACG-3′ and hCaveolin-anti 5′-ATGGTCTAGAAAGCTTATTTCTTTCTG-CAAGTTGATGCGG-3′. The resulting PCR fragment was cloned into pDNR-Dual using the In-Fusion PCR Cloning Kit (Clontech, Mountain View, CA) and transferred by Cre-mediated recombination into pLPS3′mCerulean generating caveolin-1 wild type (WT)-cerulean. pLPS3′mCerulean was generated by replacing the GFP coding sequence in pLPS3′EGFP (Creator System, Clontech) with the cDNA encoding mCerulean (Rizzo et al., 2004) generously provided by D. W. Piston (Department of Molecular Physiology and Biophysics, Vanderbilt University, Nashville, TN). Caveolin-1 G83S construct was generated by site-directed mutagenesis using the pLPS3′mCerulean caveolin-1 WT-cerulean as template and primers Cav1-G83S_sense 5′-GGGACACACAGTTTTGACTCCATATGGAAGGC-CAGCTTCACC-3′ and Cav1-G83S_anti 5′-GGTGAAGCTGGCCTTCCATATG-GAGTCAAAACTGTGTGTCCC-3′. HEK293 cells and fibroblasts were transfected with plasmids as described (Agerer et al., 2003).

Small interfering RNA transfection

To knock down the expression of caveolin-1, siRNA oligonucleotides (sense oligo: GCAAGUGUAUGACGCGCAC, antisense oligo: GUGCGCGUCAUACACUUGC) were purchased from Eurofins (Ebersberg, Germany). 2.5×10^6 NIH v-Src cells were seeded in 6 cm dishes coated with 0.1% gelatine in PBS. 100 pmol oligonucleotide was transfected per dish using INTERFERin Transfection reagent (PolyPlus-Transfection, New York, NY) following the manufacturer's instructions. As a negative control, an irrelevant oligonucleotide (SIH565859) from SABiosciences (Frederick, MD) was used.

Infection experiments, gentamicin-lysostaphin protection assay and measurement of total cell-associated bacteria

One day before infection experiments, 4×10^5 HEK293 cells or 1×10^5 fibroblasts were seeded in poly-L-lysine or gelatine-coated wells. Cells were infected with bacteria at a multiplicity of infection (MOI) of 20. For flow cytometric analysis of bacterial uptake, cells were infected with Fluorescein-labelled bacteria and analyzed as described (Pils et al., 2006). To obtain an estimate of the amount of internalized bacteria, the percentage of Fluorescein-positive cells was multiplied by the mean fluorescence intensity of these cells to obtain the uptake index (u.i.).

To evaluate intracellular bacteria by gentamicin-lysostaphin protection assay, the culture medium was replaced after infection by DMEM containing 50 μg/ml gentamicin and 20 μg/ml lysostaphin. After incubation for 1 hour at 37°C, cells were washed once with PBS and intracellular bacteria released by incubation in 1% saponin in PBS for 20 minutes at 37°C. Samples were diluted in PBS and plated on TSB agar plates for determination of the recovered colony forming units. In the case of gonococci, extracellular bacteria were killed by incubation in DMEM containing 50 μg/ml gentamicin and released intracellular bacteria were plated on GC agar plates. In inhibition experiments, pharmacological inhibitors were added to the cells 30 minutes before infection. Total cell-associated bacteria were determined in separate samples by omitting the incubation with gentamicin/lysostaphin. Cell lysis and western blotting were performed as described (Muenzner et al., 2008).

Fluorescence staining

The day before infection, 5×10^4 HEK293 cells or 3×10^4 fibroblasts were seeded on acid-washed glass-coverslips in 24-well plates. Cells were infected with fluorescently labeled staphylococci at an MOI of 50. After infection, cells were washed once with PBS and fixed with 4% paraformaldehyde for 20 minutes at room temperature. For detection of integrin β1, fixed samples were washed three times with PBS and permeabilized for 10 minutes in permeabilization buffer (PBS, 10% FCS and 0.2% saponin). Then, unspecific binding sites were saturated by incubating the samples with blocking buffer (PBS and 10% FCS) for 10 minutes. Samples were then incubated with monoclonal rat anti-integrin-β1 (AIIB2) in blocking buffer. Samples were washed twice with PBS, blocked again for 5 minutes and incubated with biotin-SP-conjugated goat anti-rat for 45 minutes at room temperature. Samples were washed again and incubated with streptavidin–Cy5. After three washes with PBS, the coverslips were mounted in embedding medium (DaKo, Glastrup, Denmark) on glass slides and sealed with nail polish. For detection of GM1, samples were treated as described for the detection of integrin β1 and then stained with either FITC- or Alexa Fluor 555-cholera-toxin B subunit (CT-FITC or CT-555). To exclusively detect surface localized GM1, the permeabilization step was omitted and this is indicated in the corresponding figure legend. Visualization of GM1 in the plasma membrane of living cells for FRAP analysis was accomplished by incubating cells with 10 μg/ml CT-FITC for 20 minutes at 37°C (Wakabayashi et al., 2005). For differentiation between extracellular and intracellular bacteria, cells were infected with Fluorescein- or Rhodamine- and biotin-labelled bacteria essentially as described (Agerer et al., 2004). Following infection and fixation, samples were blocked with PBS 10% CS without cell permeabilization and probed with streptavidin–Cy5 (Molecular Probes, Eugene, OR). Therefore, streptavidin–Cy5 reached only extracellular bacteria, resulting in Fluorescein- or Rhodamine-labelled intracellular and Fluorescein or Rhodamine and Cy5-labelled extracellular bacteria. The percentage of bacteria or beads recruiting GM1 or GPI–GFP, respectively, was determined by visually scoring all cell-associated particles for the enrichment of marker staining within 2–3 μm distance for a minimum of 20 cells each from three separate experiments.

Scanning electron microscopy, confocal microscopy and FRAP

Samples for scanning electron microscopy were prepared and analyzed as described (Muenzner et al., 2008). Fixed samples were viewed with a Leica TCS SP5 (Leica Microsystems, Wetzlar, Germany) confocal laser scanning microscope using a 63×/1.40–0.60 objective. For double- and triple-labeled fixed specimens the signals of the fluorescent dyes were serially recorded to avoid bleed-through due to simultaneous excitation. The corresponding images were digitally processed with Photoshop6 (Adobe Systems, Mountain View, CA) or ImageJ (Wayne Rasband, National Institutes of Health, USA) and merged to yield pseudo-colored RGB pictures.

For FRAP experiments, 5×10^4 CavWT and *Cav1*$^{-/-}$ cells were seeded on 35 mm 0.1% gelatine-coated glass-bottom dishes and transfected with 1.5 μg of expression plasmids using Lipofectamin2000 (Invitrogen). To measure membrane mobility in the vicinity of cell attached bacteria, cells were infected with *S. aureus* (MOI 50) for 1 hour. A defined region was bleached at full laser power (100% power, 100% transmission for 0.113 seconds) using the 488nm line of the argon laser. Recovery of fluorescence was monitored by scanning the bleached region at low laser power (100% power, 4% transmission). Images were processed using ImageJ. Quantification of FRAP experiments was performed measuring the fluorescence intensity of the bleached area before, directly after and during recovery from bleaching. Half-life time was calculated according to the following equation: $t_{1/2}=\ln(0.5)/(-\text{tau})$ and diffusion coefficient was calculated according to the following equation: $D=0.88 * w^2/(4*t_{1/2})$ (Axelrod et al., 1976).

Protein coupling to latex beads

Polybead carboxylate microspheres (Warrington, PA) were suspended in PBS and sonicated for 3 minutes. Afterwards beads were washed with PBS and resuspended in coupling buffer (0.2 M $NaHCO_3$, 0.5 M NaCl, pH 8.6). The protein was added and incubated for 2 hours at 37°C on a shaker (175 r.p.m.). Subsequently, 0.5 ml bovine serum albumin (BSA) (30 mg/ml) was added and incubated for 1 hour at 37°C and 175 r.p.m. Beads were washed with PBS, 1 mg/ml BSA and finally stored in PBS, 0.2 mg/ml BSA at 4°C. Coupled beads were incubated with human serum, which contains fibronectin, for 2 hours at room temperature. Afterwards beads were washed with flow buffer (PBS containing 5% heat-inactivated FCS, 1% sodium azide) and incubated with monoclonal anti-fibronectin antibody (clone HFN7.1). After incubation, samples were washed again and stained with a secondary Cy2-coupled antibody. Samples were analyzed by flow cytometry.

We thank Thomas F. Meyer (MPI for Infection Biology, Berlin) and Timothy J. Foster (Trinity College, Dublin, Ireland) for bacterial strains, Ludger Pelkmans (ETH Zurich, Switzerland), Ivan R. Nabi (Life Science Institute, Vancouver, Canada), Ben J. Nichols (Medical

Research Council, Cambridge, UK), Claudia A. O. Stürmer (University of Konstanz, Germany), and Ritva Tikkanen (University Clinic Frankfurt, Germany) for expression vectors of caveolin and flotillins, David W. Piston (Department of Molecular Physiology and Biophysics, Vanderbilt University, Nashville, TN) for cDNA of mCerulean, and Ludger Johannes (Institute Curie, Paris) for shiga toxin used in this study. We are indebted to M. Aoki, F. Brunk, G. D. Citieuh-Ngaleu, and J. Hentschel for analyzing samples and we thank K. Dinkla, S. Feindler-Boeckh, R. Hohenberger-Bregger, Y. Rauter, and U. Wallner for excellent technical assistance. C.H. was supported by a fellowship from the IRTG 1331. This study was supported by funds from the DFG Ha 2856/5-1 and the Center for Applied Photonics (University of Konstanz) (to C.R.H.).

Supplementary material available online at
http://jcs.biologists.org/cgi/content/full/123/24/4280/DC1

References

Agerer, F., Michel, A., Ohlsen, K. and Hauck, C. R. (2003). Integrin-mediated invasion of *Staphylococcus aureus* into human cells requires Src family protein tyrosine kinases. *J. Biol. Chem.* **278**, 42524-42531.

Agerer, F., Waeckerle, S. and Hauck, C. R. (2004). Microscopic quantification of bacterial invasion by a novel antibody-independent staining method. *J. Microbiol. Methods* **59**, 23-32.

Agerer, F., Lux, S., Michel, A., Rohde, M., Ohlsen, K. and Hauck, C. R. (2005). Cellular invasion by *Staphylococcus aureus* reveals a functional link between focal adhesion kinase and cortactin in integrin-mediated internalisation. *J. Cell Sci.* **118**, 2189-2200.

Alrutz, M. A. and Isberg, R. R. (1998). Involvement of focal adhesion kinase in invasin-mediated uptake. *Proc. Natl. Acad. Sci. USA* **95**, 13658-13663.

Axelrod, D., Koppel, D. E., Schlessinger, J., Elson, E. and Webb, W. W. (1976). Mobility measurement by analysis of fluorescence photobleaching recovery kinetics. *Biophys. J.* **16**, 1055-1069.

Bonazzi, M., Veiga, E., Pizarro-Cerda, J. and Cossart, P. (2008). Successive post-translational modifications of E-cadherin are required for InlA-mediated internalization of *Listeria monocytogenes*. *Cell. Microbiol.* **10**, 2208-2222.

Boyle, E. C. and Finlay, B. B. (2003). Bacterial pathogenesis: exploiting cellular adherence. *Curr. Opin. Cell Biol.* **15**, 633-639.

Bretscher, M. S. (1989). Endocytosis and recycling of the fibronectin receptor in CHO cells. *EMBO J.* **8**, 1341-1348.

Browman, D. T., Hoegg, M. B. and Robbins, S. M. (2007). The SPFH domain-containing proteins: more than lipid raft markers. *Trends Cell Biol.* **17**, 394-402.

Caswell, P. and Norman, J. (2008). Endocytic transport of integrins during cell migration and invasion. *Trends Cell Biol.* **18**, 257-263.

Couet, J., Li, S., Okamoto, T., Ikezu, T. and Lisanti, M. P. (1997). Identification of peptide and protein ligands for the caveolin-scaffolding domain. Implications for the interaction of caveolin with caveolae-associated proteins. *J. Biol. Chem.* **272**, 6525-6533.

Damm, E. M., Pelkmans, L., Kartenbeck, J., Mezzacasa, A., Kurzchalia, T. and Helenius, A. (2005). Clathrin- and caveolin-1-independent endocytosis: entry of simian virus 40 into cells devoid of caveolae. *J. Cell Biol.* **168**, 477-488.

del Pozo, M. A., Alderson, N. B., Kiosses, W. B., Chiang, H. H., Anderson, R. G. and Schwartz, M. A. (2004). Integrins regulate Rac targeting by internalization of membrane domains. *Science* **303**, 839-842.

del Pozo, M. A., Balasubramanian, N., Alderson, N. B., Kiosses, W. B., Grande-Garcia, A., Anderson, R. G. and Schwartz, M. A. (2005). Phospho-caveolin-1 mediates integrin-regulated membrane domain internalization. *Nat. Cell Biol.* **7**, 901-908.

Dersch, P. and Isberg, R. R. (1999). A region of the *Yersinia pseudotuberculosis* invasin protein enhances integrin-mediated uptake into mammalian cells and promotes self-association. *EMBO J.* **18**, 1199-1213.

Drab, M., Verkade, P., Elger, M., Kasper, M., Lohn, M., Lauterbach, B., Menne, J., Lindschau, C., Mende, F., Luft, F. C. et al. (2001). Loss of caveolae, vascular dysfunction, and pulmonary defects in caveolin-1 gene-disrupted mice. *Science* **293**, 2449-2452.

Dupuy, A. G. and Caron, E. (2008). Integrin-dependent phagocytosis: spreading from microadhesion to new concepts. *J. Cell Sci.* **121**, 1773-1783.

Fowler, T., Wann, E. R., Joh, D., Johansson, S., Foster, T. J. and Hook, M. (2000). Cellular invasion by *Staphylococcus aureus* involves a fibronectin bridge between the bacterial fibronectin-binding MSCRAMMs and host cell beta1 integrins. *Eur. J. Cell Biol.* **79**, 672-679.

Fowler, T., Johansson, S., Wary, K. K. and Hook, M. (2003). Src kinase has a central role in in vitro cellular internalization of *Staphylococcus aureus*. *Cell. Microbiol.* **5**, 417-426.

Frick, M., Bright, N. A., Riento, K., Bray, A., Merrified, C. and Nichols, B. J. (2007). Coassembly of flotillins induces formation of membrane microdomains, membrane curvature, and vesicle budding. *Curr. Biol.* **17**, 1151-1156.

Garner, M. J., Hayward, R. D. and Koronakis, V. (2002). The *Salmonella* pathogenicity island 1 secretion system directs cellular cholesterol redistribution during mammalian cell entry and intracellular trafficking. *Cell. Microbiol.* **4**, 153-165.

Gaus, K., Le Lay, S., Balasubramanian, N. and Schwartz, M. A. (2006). Integrin-mediated adhesion regulates membrane order. *J. Cell Biol.* **174**, 725-734.

Ghosh, P. K., Vasanji, A., Murugesan, G., Eppell, S. J., Graham, L. M. and Fox, P. L. (2002). Membrane microviscosity regulates endothelial cell motility. *Nat. Cell Biol.* **4**, 894-900.

Greene, C., McDevitt, D., Francois, P., Vaudaux, P. E., Lew, D. P. and Foster, T. J. (1995). Adhesion properties of mutants of *Staphylococcus aureus* defective in fibronectin-binding proteins and studies on the expression of fnb genes. *Mol. Microbiol.* **17**, 1143-1152.

Gulbins, E., Dreschers, S., Wilker, B. and Grassme, H. (2004). Ceramide, membrane rafts and infections. *J. Mol. Med.* **82**, 357-363.

Hauck, C. R. and Ohlsen, K. (2006). Sticky connections: extracellular matrix protein recognition and integrin-mediated cellular invasion by *Staphylococcus aureus*. *Curr. Opin. Microbiol.* **9**, 5-11.

Hauck, C. R., Hsia, D. A., Puente, X. S., Cheresh, D. A. and Schlaepfer, D. D. (2002). FRNK blocks v-Src-stimulated invasion and experimental metastases without effects on cell motility or growth. *EMBO J.* **21**, 6289-6302.

Hauck, C. R., Agerer, F., Muenzner, P. and Schmitter, T. (2006). Cellular adhesion molecules as targets for bacterial infection. *Eur. J. Cell Biol.* **85**, 235-242.

Hernandez-Deviez, D. J., Howes, M. T., Laval, S. H., Bushby, K., Hancock, J. F. and Parton, R. G. (2008). Caveolin regulates endocytosis of the muscle repair protein, dysferlin. *J. Biol. Chem.* **283**, 6476-6488.

Hynes, R. O. (2002). Integrins: bidirectional, allosteric signaling machines. *Cell* **110**, 673-687.

Kinoshita, T., Fujita, M. and Maeda, Y. (2008). Biosynthesis, remodelling and functions of mammalian GPI-anchored proteins: recent progress. *J. Biochem.* **144**, 287-294.

Kirkham, M. and Parton, R. G. (2005). Clathrin-independent endocytosis: new insights into caveolae and non-caveolar lipid raft carriers. *Biochim. Biophys. Acta* **1745**, 273-286.

Kupsch, E. M., Knepper, B., Kuroki, T., Heuer, I. and Meyer, T. F. (1993). Variable opacity (Opa) outer membrane proteins account for the cell tropisms displayed by *Neisseria gonorrhoeae* for human leukocytes and epithelial cells. *EMBO J.* **12**, 641-650.

Lafont, F. and van der Goot, F. G. (2005). Bacterial invasion via lipid rafts. *Cell. Microbiol.* **7**, 613-620.

Lafont, F., Tran Van Nhieu, G., Hanada, K., Sansonetti, P. and van der Goot, F. G. (2002). Initial steps of *Shigella* infection depend on the cholesterol/sphingolipid raft-mediated CD44-IpaB interaction. *EMBO J.* **21**, 4449-4457.

Lajoie, P., Goetz, J. G., Dennis, J. W. and Nabi, I. R. (2009a). Lattices, rafts, and scaffolds: domain regulation of receptor signaling at the plasma membrane. *J. Cell Biol.* **185**, 381-385.

Lajoie, P., Kojic, L. D., Nim, S., Li, L., Dennis, J. W. and Nabi, I. R. (2009b). Caveolin-1 regulation of dynamin-dependent, raft-mediated endocytosis of cholera toxin b-subunit occurs independently of caveolae. *J. Cell. Mol. Med.* **13**, 3218-3225.

Le, P. U., Guay, G., Altschuler, Y. and Nabi, I. R. (2002). Caveolin-1 is a negative regulator of caveolae-mediated endocytosis to the endoplasmic reticulum. *J. Biol. Chem.* **277**, 3371-3379.

Lee, W., Sodek, J. and McCulloch, C. A. (1996). Role of integrins in regulation of collagen phagocytosis by human fibroblasts. *J. Cell Physiol.* **168**, 695-704.

Leitinger, B. and Hogg, N. (2002). The involvement of lipid rafts in the regulation of integrin function. *J. Cell Sci.* **115**, 963-972.

Manninen, A., Verkade, P., Le Lay, S., Torkko, J., Kasper, M., Fullekrug, J. and Simons, K. (2005). Caveolin-1 is not essential for biosynthetic apical membrane transport. *Mol. Cell. Biol.* **25**, 10087-10096.

McNally, E. M., de Sa Moreira, E., Duggan, D. J., Bonnemann, C. G., Lisanti, M. P., Lidov, H. G., Vainzof, M., Passos-Bueno, M. R., Hoffman, E. P., Zatz, M. et al. (1998). Caveolin-3 in muscular dystrophy. *Hum. Mol. Genet.* **7**, 871-877.

Memmo, L. M. and McKeown-Longo, P. (1998). The alphavbeta5 integrin functions as an endocytic receptor for vitronectin. *J. Cell Sci.* **111**, 425-433.

Muenzner, P., Bachmann, V., Kuespert, K. and Hauck, C. R. (2008). The CEACAM1 transmembrane domain, but not the cytoplasmic domain, directs internalization of human pathogens via membrane-microdomains. *Cell. Microbiol.* **10**, 1074-1092.

Neet, K. and Hunter, T. (1995). The nonreceptor protein-tyrosine kinase CSK complexes directly with the GTPase-activating protein-associated p62 protein in cells expressing v-Src or activated c-Src. *Mol. Cell. Biol.* **15**, 4908-4920.

Neumann-Giesen, C., Falkenbach, B., Beicht, P., Claasen, S., Luers, G., Stuermer, C. A., Herzog, V. and Tikkanen, R. (2004). Membrane and raft association of reggie-1/flotillin-2: role of myristoylation, palmitoylation and oligomerization and induction of filopodia by overexpression. *Biochem. J.* **378**, 509-518.

Oggioni, M. R. and Pozzi, G. (1996). A host-vector system for heterologous gene expression in *Streptococcus gordonii*. *Gene* **169**, 85-90.

Ozeri, V., Rosenshine, I., Ben-Ze'Ev, A., Bokoch, G. M., Jou, T. S. and Hanski, E. (2001). De novo formation of focal complex-like structures in host cells by invading Streptococci. *Mol. Microbiol.* **41**, 561-573.

Pelkmans, L., Kartenbeck, J. and Helenius, A. (2001). Caveolar endocytosis of simian virus 40 reveals a new two-step vesicular-transport pathway to the ER. *Nat. Cell Biol.* **3**, 473-483.

Pils, S., Schmitter, T., Neske, F. and Hauck, C. R. (2006). Quantification of bacterial invasion into adherent cells by flow cytometry. *J. Microbiol. Methods* **65**, 301-310.

Pizarro-Cerda, J. and Cossart, P. (2006). Bacterial adhesion and entry into host cells. *Cell* **124**, 715-727.

Riethmuller, J., Riehle, A., Grassme, H. and Gulbins, E. (2006). Membrane rafts in host-pathogen interactions. *Biochim. Biophys. Acta* **1758**, 2139-2147.
Rizzo, M. A., Springer, G. H., Granada, B. and Piston, D. W. (2004). An improved cyan fluorescent protein variant useful for FRET. *Nat. Biotechnol.* **22**, 445-449.
Rohde, M., Muller, E., Chhatwal, G. S. and Talay, S. R. (2003). Host cell caveolae act as an entry-port for group A streptococci. *Cell. Microbiol.* **5**, 323-342.
Salzer, U. and Prohaska, R. (2001). Stomatin, flotillin-1, and flotillin-2 are major integral proteins of erythrocyte lipid rafts. *Blood* **97**, 1141-1143.
Sandvig, K., Garred, O., Holm, P. K. and van Deurs, B. (1993). Endocytosis and intracellular transport of protein toxins. *Biochem. Soc. Trans.* **21**, 707-711.
Sargiacomo, M., Scherer, P. E., Tang, Z., Kubler, E., Song, K. S., Sanders, M. C. and Lisanti, M. P. (1995). Oligomeric structure of caveolin: implications for caveolae membrane organization. *Proc. Natl. Acad. Sci. USA* **92**, 9407-9411.
Schmitter, T., Pils, S., Weibel, S., Agerer, F., Buntru, A., Kopp, K. and Hauck, C. R. (2007). Opa proteins of pathogenic *Neisseriae* initiate Src-kinase-dependent or lipid raft-mediated uptake via distinct human CEACAM isoforms. *Infect. Immunol.* **75**, 4116-4126.
Schwarz-Linek, U., Werner, J. M., Pickford, A. R., Gurusiddappa, S., Kim, J. H., Pilka, E. S., Briggs, J. A., Gough, T. S., Hook, M., Campbell, I. D. et al. (2003). Pathogenic bacteria attach to human fibronectin through a tandem beta-zipper. *Nature* **423**, 177-181.
Sergent, O., Pereira, M., Belhomme, C., Chevanne, M., Huc, L. and Lagadic-Gossmann, D. (2005). Role for membrane fluidity in ethanol-induced oxidative stress of primary rat hepatocytes. *J. Pharmacol. Exp. Ther.* **313**, 104-111.
Seveau, S., Bierne, H., Giroux, S., Prevost, M. C. and Cossart, P. (2004). Role of lipid rafts in E-cadherin- and HGF-R/Met-mediated entry of *Listeria monocytogenes* into host cells. *J. Cell Biol.* **166**, 743-753.
Shi, F. and Sottile, J. (2008). Caveolin-1-dependent {beta}1 integrin endocytosis is a critical regulator of fibronectin turnover. *J. Cell Sci.* **121**, 2360-2371.
Sinha, B., Francois, P. P., Nusse, O., Foti, M., Hartford, O. M., Vaudaux, P., Foster, T. J., Lew, D. P., Herrmann, M. and Krause, K. H. (1999). Fibronectin-binding protein acts as *Staphylococcus aureus* invasin via fibronectin bridging to integrin alpha5beta1. *Cell. Microbiol.* **1**, 101-117.
Solis, G. P., Hoegg, M., Munderloh, C., Schrock, Y., Malaga-Trillo, E., Rivera-Milla, E. and Stuermer, C. A. (2007). Reggie/flotillin proteins are organized into stable tetramers in membrane microdomains. *Biochem. J.* **403**, 313-322.
Sotgia, F., Razani, B., Bonuccelli, G., Schubert, W., Battista, M., Lee, H., Capozza, F., Schubert, A. L., Minetti, C., Buckley, J. T. et al. (2002). Intracellular retention of glycosylphosphatidyl inositol-linked proteins in caveolin-deficient cells. *Mol. Cell. Biol.* **22**, 3905-3926.
Sottile, J. and Chandler, J. (2005). Fibronectin matrix turnover occurs through a caveolin-1-dependent process. *Mol. Biol. Cell* **16**, 757-768.
Talay, S. R., Zock, A., Rohde, M., Molinari, G., Oggioni, M., Pozzi, G., Guzman, C. A. and Chhatwal, G. S. (2000). Co-operative binding of human fibronectin to Sfbl protein triggers streptococcal invasion into respiratory epithelial cells. *Cell. Microbiol.* **2**, 521-535.
Tsuda, K., Furuta, N., Inaba, H., Kawai, S., Hanada, K., Yoshimori, T. and Amano, A. (2008). Functional analysis of alpha5beta1 integrin and lipid rafts in invasion of epithelial cells by *Porphyromonas gingivalis* using fluorescent beads coated with bacterial membrane vesicles. *Cell Struct. Funct.* **33**, 123-132.
van der Flier, A. and Sonnenberg, A. (2001). Function and interactions of integrins. *Cell Tissue Res.* **305**, 285-298.
van Putten, J. P., Duensing, T. D. and Cole, R. L. (1998). Entry of OpaA+ gonococci into HEp-2 cells requires concerted action of glycosaminoglycans, fibronectin and integrin receptors. *Mol. Microbiol.* **29**, 369-379.
van Zanten, T. S., Cambi, A., Koopman, M., Joosten, B., Figdor, C. G. and Garcia-Parajo, M. F. (2009). Hotspots of GPI-anchored proteins and integrin nanoclusters function as nucleation sites for cell adhesion. *Proc. Natl. Acad. Sci. USA* **106**, 18557-18562.
Wakabayashi, M., Okada, T., Kozutsumi, Y. and Matsuzaki, K. (2005). GM1 ganglioside-mediated accumulation of amyloid beta-protein on cell membranes. *Biochem. Biophys. Res. Commun.* **328**, 1019-1023.
Wary, K. K., Mariotti, A., Zurzolo, C. and Giancotti, F. G. (1998). A requirement for caveolin-1 and associated kinase Fyn in integrin signaling and anchorage-dependent cell growth. *Cell* **94**, 625-634.

Journal of Cell Science